Molecular structure, magnetic properties, cyclic voltammetry of the low-spin iron(III) Bis(4-ethylaniline) complex with the para -chloro substituted meso -tetraphenylporphyrin

Selma Dhifaoui, Chadlia Mchiri, Pierre Quatremare, Valerie Marvaud, Anna Bujacz, Habib Nasri

Molecular structure, magnetic properties, cyclic voltammetry of the low-spin iron(III) Bis(4-ethylaniline) complex with the *para*-chloro substituted *meso*-tetraphenylporphyrin

Selma Dhifaoui [a], Chadlia Mchiri [a], Pierre Quatremare [b], Valérie Marvaud [b], Anna Bujacz [c], Habib Nasri [a,*]

[a] University of Monastir, Laboratoire de Physico-chimie des Matériaux, Faculté des Sciences de Monastir, Avenue de L 'environnement, 5019, Monastir, Tunisia
[b] IPCM, Institut Parisien de Chimie Moléculaire, UPMC, Sorbonne Université, 4 Place Jussieu, 75252 Paris Cedex 0, France
[c] X-Ray Analysis Laboratory, Institute of Technical Biochemistry, Lodz University of Technology, Stefanowskiego 4/10, 90-924 Lodz, Poland

ARTICLE INFO

Article history:
Received 11 August 2017
Received in revised form
5 October 2017
Accepted 6 October 2017
Available online 9 October 2017

Keywords:
Iron(III) porphyrins
X-ray molecular structure
UV–Visible
Magnetic data

ABSTRACT

In this study, the preparation of a new iron(III) hexacoordinated metalloporphyrin namely the bis(4-ethylaniline)(*meso*-tetra(*para*-chlorophenyl)porphyrinato)iron(III) triflate hemi-4-ethylaniline monohydrate with the formula $[Fe^{III}(TClPP)(PhEtNH_2)_2]SO_3CF_3 1/2PhEtNH_2 H_2O$ (I) was reported. This is the first example of an iron(III) metalloporphyrin bis(primary amine) with an aryl group adjacent to the amino group. This species was characterized by elemental, spectroscopic analysis including UV–visible and IR data, cyclic voltammetry, SQUID measurements and X-ray molecular structure. The mean equatorial distance between the iron(III) and the nitrogens of the porphyrin is appropriate for a low-spin (S = 1/2) iron(III) porphyrin complex. The magnetic data confirm the low-spin state of our ferric derivative while the cyclic voltammetry indicates a shift of the half potential $E_{1/2}$[Fe(III)/Fe(II)] of complex (I) toward more negative value. In the crystal of (I), the $[Fe^{III}(TClPP)(PhEtNH_2)_2]^+$ ions, the triflate counterions and the water molecules are involved in a number of O–H···O, N–H···O, C–H···O and C–H···π intermolecular interactions forming a three-dimension network.

1. Introduction

During the late sixties and the seventies of the last century, several investigations were carried out on iron(III) metallporphyrins with aliphatic amines leading to the autoreduction of the central metal [1,2]. Later on, Catro et al., reported that only sterically unhindered alkylamines are capable of reducing ferric porphyrins [3]. Several ferrous bis(primary amine) porphyrins were prepared by reduction of iron(III) porphyrinic ion complexes by primary amines with C-H proton adjacent to the NH_2 group [4]. This is the case of the $[Fe^{II}(TPP)(RNH_2)_2]$ coordination compounds where RNH_2 = 1-butylamine, benzylamine, and phenethylamine [4]. More recently we reported the preparation, the spectroscopic and structural characterizations of two iron(II) bis(primary amine) complexes $[Fe^{II}(TClPP)(BzNH_2)_2]$ ($BzNH_2$ = benzylamine [5] and $[Fe^{II}(TMPP)(amp)_2]$ (TMPP = tetrakis(4-metoxyphenyl)porphyrinato and amp = 4-(2-Aminoethyl)morpholine) by reacting iron(III) triflato starting materials $[Fe^{III}(Porph)(SO_3CF_3)]$ (Porph = porphyrin) with an excess of primary amines [6]. It is noteworthy that a very limited number of bis(amine) ferric metalloporphyrins is reported in the literature compared to the bis(primary amine) ferrous porphyrins. These iron(III) hexa-coordinated species only have been observed at low temperature or in high dilution [7,8]. Simonneaux et al. [9], reported for the first time the complete characterization of a bis(amine ester) ferric species $[Fe^{III}(TPP)(NH_2CHR)_2]SO_3CF_3$ (with NH_2CHR = L-leucine methyl ester: $NH_2CH(CO_2CH_3)(CH(CH_3)_2)$. In 2002, the same author reported the molecular structure of another bis(amine ester) namely the bis(L-valine-methyl ester)(*meso*-tetraphenylporphyrinato) iron(III) ion complex [10]. In this paper, we describe the preparation, the UV–visible and IR spectroscopic characterization, the magnetic data, the cyclic voltammetry results and the molecular structure of the first example of an iron(III) bis(primary amine) with an aryl group adjacent to the NH_2 group. This type of

* Corresponding author.
E-mail addresses: hnasri1@gmail.com, habib.nasri@fsm.rnu.tn (H. Nasri).

coordination compound is relevant to the membrane-embedded cytochrome *f* from turnip chloroplast which has an unprecedented axial heme iron ligand: the amino terminus of the polypeptide chain [11].

2. Experimental section

2.1. Materials and methods

All reagents employed were commercially available and were used as received without further purification. The *meso*-tetra(*para*-chlorophenyl)porphyrin (H_2TClPP) were prepared by using the Alder and Longo method [12]. All reactions and manipulations for the preparation of the ferric porphyrin derivatives were carried out under aerobic conditions. The chloro and the triflato iron(III) starting materials has been prepared using the literature reported methods [13,14]. Fourier-transformer IR spectra were recorded on a PerkinElmer Spectrum Two FT-IR spectrometer and UV–visible spectra were recorded with a WinASPECT PLUS (validation for SPECORD PLUS version 4.2). Cyclic voltammetry (CV) experiment was performed with a CH-660B potentiostat (CH Instruments) at room temperature under an argon atmosphere in a standard one-compartment, three-electrode electrochemical cell. Tetra-*n*-butylammonium hexafluorophosphate ($TBAPF_6$) was used as the supporting electrolyte (0.2 M) in dichloromethane previously distilled over calcium hydride under argon. An automatic Ohmic drop compensation procedure was systematically implemented before the CV data were recorded with electrolytic solution containing the studied compound at concentration of ca. 10^{-3} M. CH Instruments vitreous carbon (($Ø = 2$ mm) working electrodes were polished with 1 μm diamond paste before each recording. The saturated calomel electrode SCE ($TBAPF_6$ 0.2 M in CH_2Cl_2) redox couple was used as the reference electrode. The potential of the ferrocene/ferrocenium redox couple was used as an internal reference (0.37 V/SCE experimental conditions). Temperature-dependent magnetic susceptibility measurements on polycrystalline sample of (**I**) was made using a Quantum Design MPMS-5SSQUID magnetometer over a temperature range of 2–300 K at a measuring field of 0.1 T. Magnetization versus magnetic field measurements of (**I**) were carried out at 2.0 K in the field range 0–5 T. The amount of material used for the measurements was 12.86 mg. Diamagnetic correction of the constituent atoms of (**I**) was estimated from Pascal constants [15] with value -351.10^{-6} cm^3 mol^{-1}.

2.2. Preparation of complex (*I*)

2.2.1. Synthesis of $[Fe^{III}(TClPPP)(PhEtNH_2)_2]SO_3CF_3$ 1/2($PhEtNH_2$) H_2O (*I*)

$[Fe^{III}(TClPP)(SO_3CF_3)]$ (50 mg, 0.05 mmol) and 4-ethylaniline (100 mg, 0.60 mmol) were dissolved in dichloromethane (10 mL). The mixture was stirred at room temperature for 4 h. The solution was filtered, and crystals of the complex were prepared by slow diffusion of n-hexane into the dichloromethane solution. Yield 10 mg, 0.01 mmol (20%). $C_{65}H_{53.5}Cl_4F_3FeN_{6.5}O_4S$ (1276.35); Calcd. C 61.16; H 4.22; N 7.13; Found: C 61.25; H 4.31; N 7.26; UV–visible [CH_2Cl_2]: λ_{max} ($\varepsilon.10^{-3}$): 416 (265), 555 (18) nm.

2.3. X-ray structure determination

The data collection for (**I**) was performed with a Bruker APEXII CCD Gemini ultra-diffractometer equipped with Cu-$K\alpha$ radiation source ($\lambda = 1.54184$ Å). The intensity data was collected by the narrow frame method and the measurements of the data were done at 100 K. The reflections were scaled and corrected for absorption effects by using the Crys Alis [16]. The structure was solved by direct methods by using SIR-2004 [17] and refined by full-matrix least-squares techniques on F^2 by using the SHELXL-2014 program [18]. The crystallographic data and structural refinement details of complex (**I**) are shown in Table 1.

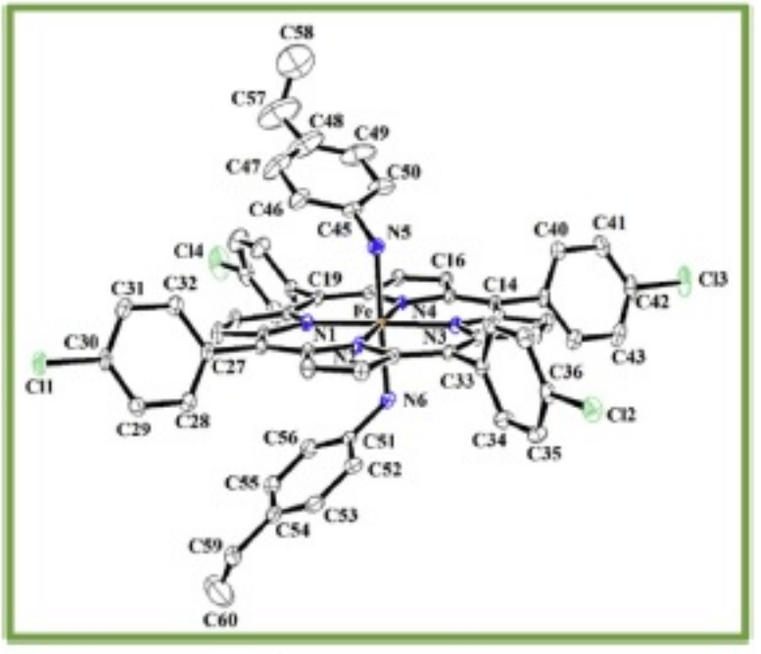

Fig. 1. ORTEP diagram of the $[Fe^{III}(TClPP)(PhEtNH_2)_2]^+$ ion complex (**I**). Ellipsoids are drawn at 40% and the hydrogen atoms are omitted for clarity.

3. Results and discussion

3.1. Structural properties of $[Fe^{III}(TClPPP)(PhEtNH_2)_2]SO_3CF_3$1/2($PhEtNH_2$) $*H_2O$ (*I*)

Complex (**I**) crystallizes in the monoclinic crystal system ($P2_1/n$

Table 1
Crystal data and structural refinement for $[Fe^{III}(TClPPP)(PhEtNH_2)_2]SO_3CF_3$1/2($PhEtNH_2$) $*H_2O$ (**I**).

Formula	$C_{65}H_{53.5}Cl_4F_3FeN_{6.5}O_4S$
Dcalc./g cm^{-3}	1.446
μ(mm^{-1})	0.481
Formula Weight	1276.35
Colour	brown
Shape	block
Size/mm^3	0.40 × 0.22 x 0.12
T(K)	100(2) K
Crystal System	monoclinic
Space Group	P $2_1/n$
a (Å)	16.4360(3)
b (Å)	15.4960(3)
c (Å)	23.1719(4)
α(°)	90
β(°)	96.513(2)
δ (°)	90
V(Å^3)	5863.61(19)
Z	4
F000 (Å^3)	2632
radiation-type	CuKα
θmin (°)	3.438
θmax (°)	75.096
Reflections measured	45088
Independent reflections	8365
Parameters	853
GooF (S)	1.028
R_1 (all data)	0.0411
wR_2 (all data)	0.1053
CCDC	1563523

[a]: $R_1 = \Sigma||Fo| - |Fc||/\Sigma|Fo|$. [b]$wR_2 = \{\Sigma[w(|Fo|^2 - |Fc|^2)^2]/\Sigma[w(|Fo|^2)^2]\}^{1/2}$.

Table 2
Selected bond lengths and angles for $[Fe^{III}(TClPPP)(PhEtNH_2)_2]SO_3CF_3^-1/2(PhEtNH_2)$ $^*H_2O$ (I).

Distances (Å)		Angles (°)	
Iron(III) coordination polyhedron			
Fe–N1	1.9814(16)	N1-Fe-N2	89.84(6)
Fe–N2	1.9952(16)	N1-Fe-N4	90.40(6
Fe–N3	1.9926(15)	N1-Fe-N3	179.27(6)
Fe-N4	1.9968(16)	N5-Fe-N6	177.82(6)
Fe-N5	2.0435(16)		
Fe-N6	2.0465(16)		
4-ethylaniline axial ligand			
C45-N5	1.443(2)	C51-N6-Fe1	120.90
C51-N6	1.440(2)	C56-C51-C52	119.99(19)
C51-C56	1.387(3)		
C51-C56	1.387(3)		

space group). The iron(III) cation is coordinated by four pyrrole N atoms of the porphyrin macrocycle and the nitrogen atoms of two *trans* 4-ethylaniline axial ligands in an octahedral geometry. The asymmetric unit of our iron(III) derivative is made by one $[Fe^{III}(TClPPP)(PhEtNH_2)_2]^+$ ion complex and $SO_3CF_3^-$ counterion, half non-coordinated $PhEtNH_2$ molecule and one water molecule. An ORTEP drawing of the $[Fe^{III}(TClPP)(PhEtNH_2)_2]^+$ ion complex is illustrated by Fig. 1. Selected bond distances and angles for this compound are listed in Table 2.

The distance between the central metal and the nitrogen atom of the $PhEtNH_2$ axial ligand is 2.045(16) Å which is close to those of the related bis(primary amine) iron(II) porphyrins type $[Fe(TPP)(RNH_2)_2]$ [4]. It has been shown that the average equatorial distance between the iron(III) and the nitrogen atoms of the porphyrin ring (Fe—Np) is related to the spin-state of the ferric metalloporphyrin [19]. Thereby, for high-spin (HS) (S = 5/2) complexes, the Fe—Np bond length values are the longest (Table 3), e.g. for the $[Fe(TPP)(H_2O)_2]^+$ ion complex, Fe—Np amounts to 2.045 Å [20]. For iron(III) low-spin (LS) (S = 1/2) metalloporphyrins, the Fe—Np bond values are smaller than those of the HS species and range between 1.998 Å and 1.952 Å. For (I), the Fe—Np distance of 1.9915(16) Å is an indication that this species is an iron(III) low-spin (S = 1/2) porphyrin complex.

The porphyrin macrocycle of (I) presents a nearly planar confirmation with maximum and minimum deviation from the $C_{20}N_4$ mean plan of 0.15(17) Å and −0.12(24) Å for atom C1 and C17 respectively while the iron(III) central metal is practically in the central of this mean plane (Fig. SI-2). For the related 4-cyanopyridine with the *meso*-tetraphenylporphyrin ion complex $[Fe^{III}(TPP)(4\text{-}CNpy)_2]^+$ [21], the porphyrin core is very distorted due to the interaction between the ortho hydrogens of the 4-cyanopyridine axial ligands and the nitrogen of the porphyrin macrocycle with a distance of ~2.52 Å. Therefore, these ortho H of the 4-CNpy axial ligand point away from the pyrrole nitrogens (Fig. 2). For our bis(4-ethylaniline)-iron(III) derivative, due to the presence of the amino group of the $PhEtNH_2$ axial ligand, the interaction between the ortho H atoms of the phenyl group of the axial ligand and the nitrogen of the pyrroles is weaker compared to the bis(4-CNpy) iron(III) species with a distance between the closest porphyrin nitrogen and the ortho H of the primary amine axial ligand of about 3.00 Å. Consequently, the ortho protons of the axial ligands nearly eclipse the closest Fe—Np vectors and le porphyrin core of (I) is rather planar.

A $[Fe^{III}(TClPPP)(PhEtNH_2)_2]^+$ ion complex is linked to a $SO_3CF_3^-$ counterion and a water molecule via N—H···O hydrogen bonds with a N5—H5···O1 and N6—H6···O4 distances of 3.119(7) Å and 2.962(2)

Table 3
Selected structural features of several six-coordinates iron(III) and iron(II) metalloporphyrins.

Complex	Fe–Np[a] (Å)	Fe–Lax[b] (Å)	Stat Spin	Ref.
Iron(III) metalloporphyrins				
$[Fe(TPP)(F)_2]^+$[c]	2.064	1.966	5/2	[22]
$[Fe(OEP)(DMSO)_2]^+$[d,e]	2.037	2.083	5/2	[23]
$[Fe(TPP)(H_2O)_2]^+$	2.045	2.095	5/2	[19]
$[Fe(TPP)(4\text{-}MeHIm)_2]^+$[f]	1.998	1.928/1.958	1/2	[24]
$[Fe(TPP)(py)_2]^+$	1.982	2.005/2.001	1/2	[25]
$[Fe(TPP)(4\text{-}CNPy)_2]^+$[g]	1.952(7)	2.002(8)	1/2	[26]
$[Fe(OEP)(3\text{-}ClPy)_2]^+$[h]	1.994(2)	2.031(2)	1/2	[27]
$[Fe(TMP)(1\text{-}MeIm)_2]^+$[i,j]	1.988(20)	1.973(6) 1.957(6)	1/2	[21]
$[Fe(TMP)(4\text{-}NMe_2Py)_2]^+$[k]	1.964(4)	1.989(4)	1/2	[21]
$[Fe(TPP)(C_6H_{13}NO_2)_2]^+$[l]	1.997(2)	2.024(2)	1/2	[10]
$[Fe(TClPPP)(PhEtNH_2)_2]^+$	1.9915(14)	2.045(16)	1/2	this work
Iron(II) metalloporphyrins				
$[Fe(TMPP)(amp)_2]$[m,n]	1.988(2)	2.037(2)	0	[7]
$[Fe(TPP)(1\text{-}BuNH_2)_2]$[o]	1.989(1)	2.039(3)	0	[4]
$[Fe(TPP)(BzNH_2)_2]$[p]	1.992(4)	2.043(3)	0	[4]
$[Fe(TPP)(PhCH_2CH_2NH_2)_2]$[q]	1.989(4)	2.028(2)	0	[4]

[a] Fe—Np = average equatorial distance between the iron and the nitrogen atoms of the porphyrin ring.
[b] Fe—Lax = iron-axial ligand distance.
[c] TPP = meso-tetraphenylporphyrinato.
[d] OEP = octaethylporphyrinato.
[e] DMSO = dimethylsulfoxide.
[f] 4-MeHIm = 4-methylimidazole.
[g] 4-CNpy = 4-cyanopyridine.
[h] 3-Clpy = 3-chloropyridine.
[i] TMP = meso-tetramesitylporhyrinato.
[j] 1-MeHIm = 1-methylimidazole.
[k] $4\text{-}NMe_2py$ = 4-(dimethylamino)pyridine.
[l] $C_6H_{13}NO_2$ = L-valine-N methyl ester.
[m] Tetrakis(4-metoxyphenyl) porphyrinatol.
[n] amp = 4-(2-aminoethyl)morpholine.
[o] $1\text{-}BuNH_2$ = 1-butylamine.
[p] $BzNH_2$ = benzylamine.
[q] $PhCH_2CH_2NH_2$ = phenethylamine.

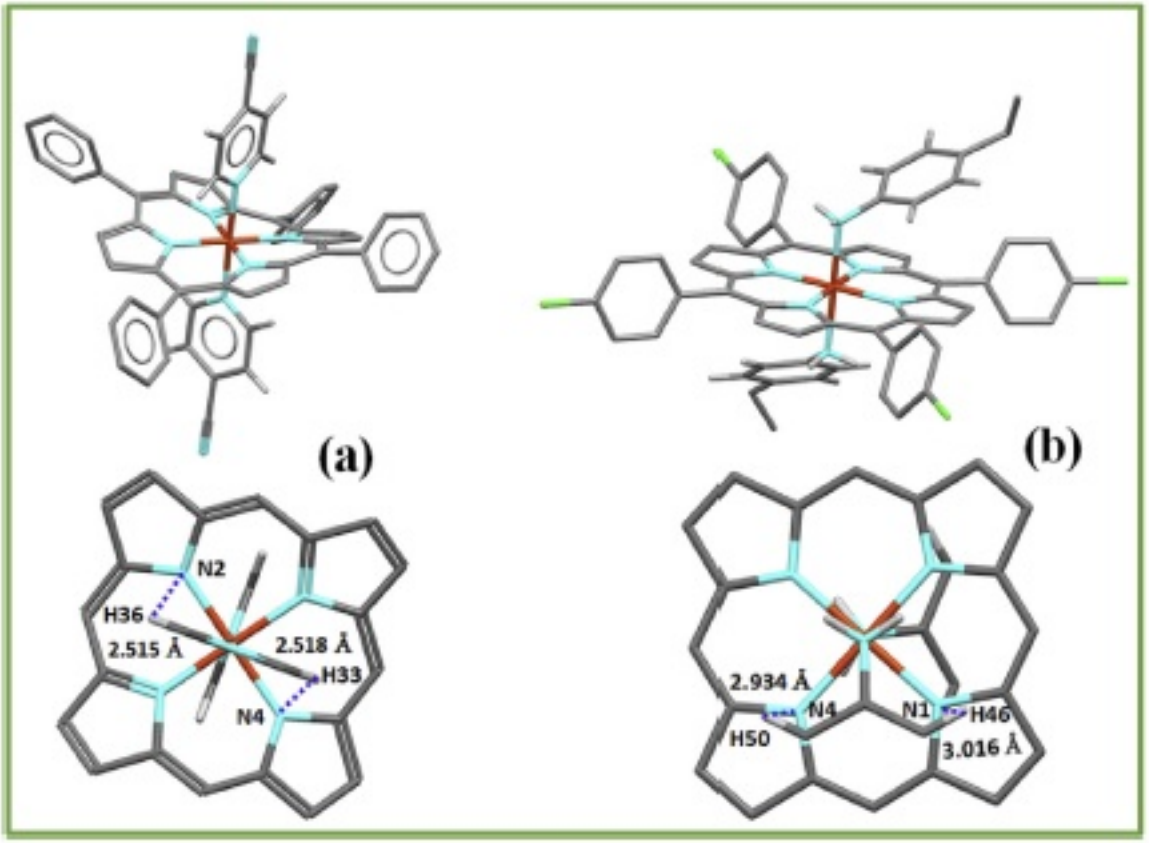

Fig. 2. Drawing showing the deformation of the porphyrin macrocycle (top view) and the interactions between the nitrogen atoms of the porphyrin ring and the H ortho of the axial ligands (bottom view) for: (a) $[Fe^{III}(TPP)(4\text{-}CNpy)_2]^+$ [21] and (b) $[Fe^{III}(TClPP)(PhEtNH_2)_2]^+$ (I). For our ion complex (I), only the NH_2 group and the ortho H of the 4-ethylaniline are shown.

Å respectively. The counterion and the nearby water molecule are linked together via the oxygen O4 of this water molecule and the oxygen atom O2 of the $SO_3CF_3^-$ counterion [O4–H4···O2 distance is 2.897(5) Å] (Fig. 2, Fig. SI-3 and Tables SI–1). By the other hand, the carbon C30 of a phenyl ring of a TClPP moiety and the oxygen O3 of a neighboring $SO_3CF_3^-$ counterion are weakly bonded via a C–H···O non-conventional H bond with a C31–H31···O3 distance of 3.475(7) Å (Fig. 3 and Fig. SI-3). The three-dimensional

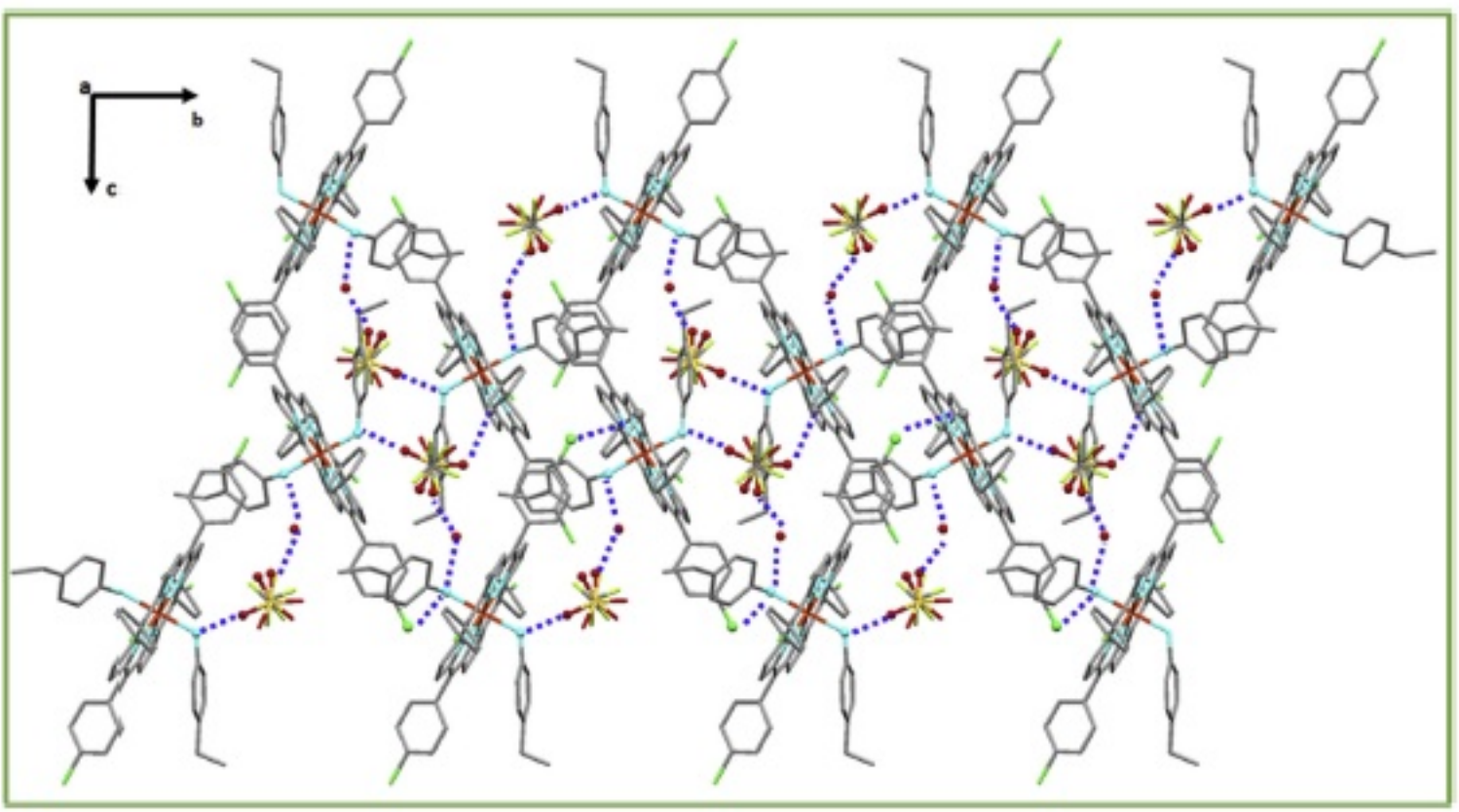

Fig. 3. A partial view of the crystal packing of the title compound plotted in projection along the [100] direction.

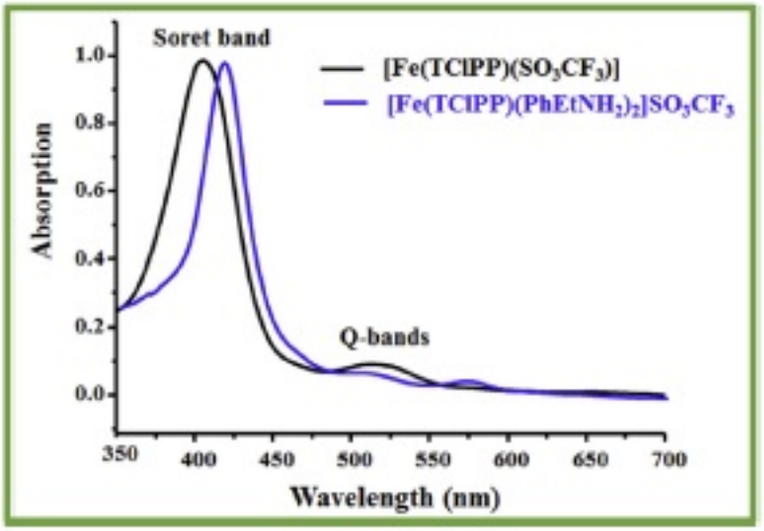

Fig. 4. UV–visible absorption spectra of the $[Fe^{III}(TClPP)(SO_3CF_3)]$ starting material and complex (I) in CH_2Cl_2 solution at concentrations of $2.08.10^{-6}$ for $[Fe^{III}(TClPP)(SO_3CF_3)]$ and $1.75.10^{-6}$ for (I).

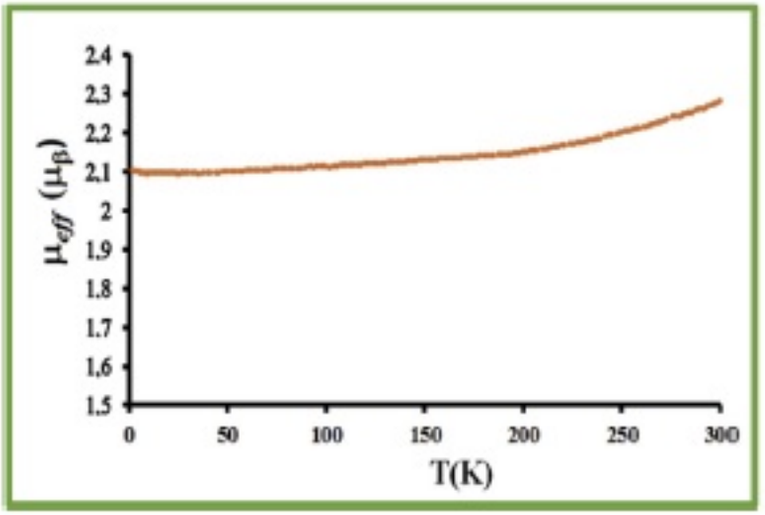

Fig. 5. Temperature dependence of the effective magnetic moment (μ_{eff}) of complex (I).

supramolecular structure of (I) is further stabilized by the C–H ... Cg intermolecular interactions between the C11 carbon of a pyrrole ring of one TClPP porphyrinato and the centroid Cg14 of the phenyl group of the 4-ethylaniline of an adjacent $[Fe^{III}(TClPPP)(PhEtNH_2)_2]^+$ ion complex (Fig. SI-3).

3.2. UV–visible and IR

Fig. 4 represents the UV–visible spectra of (I) and the $[Fe^{III}(TClPP)(SO_3CF_3)]$ starting material. The λ_{max} value of the Soret band of our iron(III)-bis(4-ethylaniline) which is 416 nm is redshifted compared to iron(III)-triflato starting material but very close to those of the iron(III)-bis(amine primary) *meso*-tetraphenylporphyrins $[Fe^{III}(TPP)(NH_2CHR)_2]^+$ related species [7] and other bis(substituted pyridine) and bis(substituted imidazole) iron(III) metalloporphyrins (Table 4). Thus, the UV–visible data of (I) indicate that in dichloromethane solution our Fe(III) derivative is hexacoordinated type $[Fe^{III}(Porph)(L)_2]^+$ where Porph is a *meso*-porphyrin and L is a neutral N-donor axial ligand.

The IR spectrum of our iron(III) derivative (Fig. SI-1) exhibits strong absorption bands at 3122 and 1613 cm^{-1}, attributed to the N-H and the C-H stretching frequency respectively of the 4-ethylaniline axial ligand. The presence of the triflate counterion is confirmed by three absorption bands at 1256, 1153 and 626 cm^{-1} [14]. Thereby, the IR results confirm the presence of the 4-ethylaniline axial ligand and the $SO_3CF_3^-$ counterion.

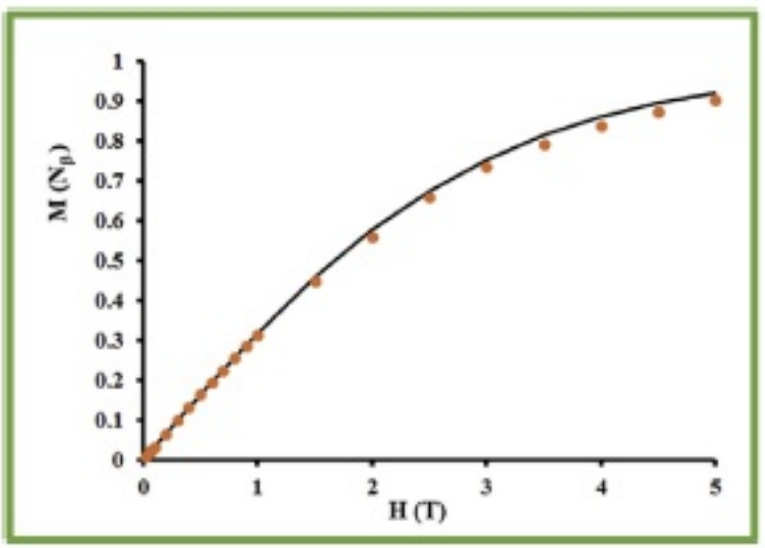

Fig. 6. Magnetization versus the applied magnetic field at 2.0 K. (●) experimental data of (I). The black line is the Brillouin function with g = 2.

3.3. Magnetic data

Magnetic properties were investigated for complex (I) via SQUID magnetometry over the temperature range 2–300 K. Plots of the effective magnetic moment (μ_{eff}) versus the temperature of the polycrystalline samples are illustrated in Fig. 5. The μ_{eff} values at 2.0 K and 300 K are 2.10 μ_β and 2.30 μ_β respectively which are

Table 4
UV–visible data of our synthetic species and selected iron(III) metalloporphyrins.

Compound	Soret band λ_{max} [nm] (ε 10^{-3} (L mol^{-1} cm^{-1}))	Q bands λ_{max} [nm] (ε 10^{-3} (L mol^{-1} cm^{-1}))	Ref.
H_2TClPP	420 (340)	515 (23), 548 (11), 593 (7), 646 (4)	this work
$[Fe(TClPP)(SO_3CF_3)]$	406 (106)	515 (11)	this work
$[Fe(TClPP)(PhEtNH_2)_2]^+$[a] (I)	416 (265)	555 (18)	this work
$[Fe^{III}(TPP)(NH_2CHR)_2]^+$[b,c]	415	541, 571	[7]
$[Fe^{III}(TMP)(4\text{-}NMePy)_2]^+$[d,e]	415	554, 588	[28]
$[Fe(TMP)(2\text{-}MeIm)_2]^+$[f]	417	560, 582	[28]
$[Fe(TMP)(1\text{-}MeIm)_2]^+$[g]	416	550, 580	[28]

[a] $PhEtNH_2$ = 4-ethylaniline.
[b] TPP = meso-tetraphenylporphyrinato.
[c] NH_2CHR = L-leucine methyl ester.
[d] TMP = meso-tetramesitylporhyrinato.
[e] 4-NMePy = 4-(dimethylamino)pyridine.
[f] 2-MeHIm = 2-methylimidazole.
[g] 1-MeHIm = 2-methylimidazole.

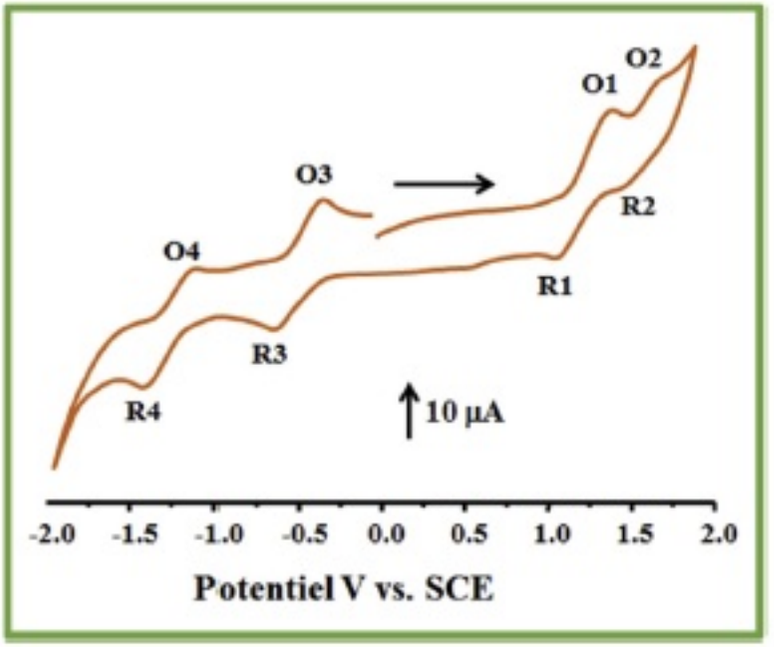

Fig. 7. Cyclic voltammogram of (I). The solvent is CH_2Cl_2 and the concentration is ca. 10^{-3} M in 0.2 M $TBAPF_6$, 100 mV/s, vitreous carbon working electrode (Ø = 2 mm).

appropriate for low-spin (S = 1/2) iron(III) compounds with g = 2. Increasing the temperature results in a gradual increase in the magnetic moment. This increase can arise from cooperative interactions between the $[Fe^{III}(TClPP)(PhEtNH_2)_2]^+$ ion complexes [29]. The field dependence of the magnetization, M = f(H) at 2 K is given in Fig. 6. The experimental magnetization (M) values are compatible with the theoretical ones calculated from the Brillouin function for S = 1/2 ground state and g = 2 for (I).

3.4. Cyclic voltammetry

The electrochemical behavior of (I) was studied by cyclic voltammetry (CV) with tetra-*n*-butylammonium hexafluorophosphate ($TBAPF_6$) as the supporting electrolyte (0.2 M) in the non-coordinating solvent dichloromethane under an argon atmosphere. The CV of the species are illustrated in Fig. 7 and the values of the half potential waves of our derivative along with other related iron(III) metalloporphyrins are given in Table 5. The anodic part of the cyclic voltammogram of (I) includes one electron reversible oxidation wave of the iron [Fe(III)/Fe(IV)] (R1/O1) with $E_{1/2}$ value of 1.11 V and a second one-electron irreversible oxidation wave (O2/R2) attributed to the oxidation of the porphyrin ring where the $E_{1/2}$ value is ~1.60 V. The cathodic part of the CV exhibits one-electron reversible reduction wave of the Fe(III) to Fe(II) (R3/O3) with a half-potential value of −0.38 V while the one-electron reversible reduction (R4/O4) wave at $E_{1/2}$ ~ −1.23 V could be attributed to the Fe(II)/Fe(I) reduction. In the literature, several investigations by cyclic voltammetry on the Fe(III)/Fe(II) reduction of ferric metalloporphyrins have been reported [30,31] and attempts have been made to correlate the changes of the $E_{1/2}$ [Fe(III)/Fe(II)] value with metal spin state, axial-ligand coordination, basicity of the porphyrin ring, counterion and the deformation of the porphyrin core. For low-spin Fe(III) porphyrin species type $[Fe^{III}(Porph)(L)_2]^+$, (Porph = *meso* or β-pyrrole substituted porphyrin), where L is a N-donor neutral planar axial ligand, it has been noticed that the shift of the $E_{1/2}$[Fe(III)/Fe(II)] toward more positive values is related to distortion of the porphyrin core. Thus, in the case of $[Fe^{III}\{(TPP)(2–6F)\}(py)_2]^+$ where {(TPP)(2–6F)} is the *meso*-tetrakis(2,6-difluorophenyl)porphyrinato, the half-potential of the Fe(III)/Fe(II) reduction is 0.35 V [32]. In contrast, the $[Fe^{III}(OEP)(1\text{-}NMeIm)_2)]^+$ ion complex (OEP = octaethylporphyrin and 1-NMeIm = 1-methylimidazole), the $E_{1/2}$[Fe(III)/Fe(II)] value is −0.39 V for which the porphyrin macrocycle of the OEP porphyrinate is practically planar [33]. For our iron(III)-TClPP bis(4-ethylaniline) complex, the $E_{1/2}$ [Fe(III)/Fe(II)] value is −0.38 V. This is compatible with a ferric hexa-coordinated metalloporphyrin with planar porphyrin core which is the case of (I) (see crystallographic section).

Table 5
Electrochemical data[a] for (I) and a selection of related iron(III) metalloporphyrins in CH_2Cl_2 (exceptions are indicated).

Complex	Ring oxidation	Oxidations	Reductions		Ref.
		Fe(III)/Fe(IV)	Fe(III)/Fe(II)	Fe(II)/Fe(I)	
		$E_{1/2}$[b]	$E_{1/2}$	$E_{1/2}$	
$[Fe^{III}(TPP)(4\text{-}CNpy)_2]^+$[c,d,e]	–	–	0.34	–	[32]
$[Fe^{III}(TPP)(1\text{-}NMeIm)_2]^+$[f]	–	–	−0.089	–	[32]
$[Fe^{III}\{(TPP)(2–6)\}(py)_2]^+$[g]	–	–	0.35	–	[32]
$[Fe^{III}(OEP)(py)_2)]^+$[h]	–	–	−0.16	–	[33]
$[Fe^{III}(OEP)(NMeIm)_2)]^+$[i]	–	–	−0.39	–	[33]
$[Fe^{III}(OEP)(4\text{-}NH_2Py)_2)]^+$[j]		–	−0.39	–	[33]
$[Fe^{III}(OEP)(pyz)_2)]^+$[k]	1.59	1.23	−0.20	–	[31]
$[Fe^{III}(TMP)(NMeIm)_2]^+$[l]	–	–	−0.27	–	[32]
$[Fe^{III}(TMP)(1\text{-}MeIm)_2]^+$	–	–	−0.27	–	[32]
$[Fe^{III}(TMP)(2\text{-}MeIm)_2]^+$[m]	–	–	−0.21	–	[32]
$[Fe^{III}(TClPPP)(PhEtNH_2)_2]$ (I)	1.60	1.11	−0.38	−1.23	this work

[a] The potentials are reported versus SCE.
[b] $E_{1/2}$ = half-wave potential.
[c] TPP = meso-tetraphenylporphyrinato.
[d] In DMF solvent.
[e] 4-CNpy = 4-cyanopyridine.
[f] 1-MeHIm = 1-methylimidazole.
[g] {(TPP)(2–6F)} = meso-tetrakis(2,6-difluorophenyl)porphyrinato.
[h] OEP = octaethylporphyrinato.
[i] NMeHIm = N-methylimidazole.
[j] 4-NH_2Py = 4-aminopyridine).
[k] pyz = pyrazine.
[l] TMP = meso-tetramesitylporhyrinato.
[m] 2-MeHIm = 2-methylimidazole.

4. Conclusion

The synthesis, the molecular structure, the magnetic, the UV–visible, the IR and the cyclic voltammetry data of a new hexa-coordinated ferric complex bearing N-donor axial ligand with an alpha aryl carbon of an amino group (I) is reported herein using the *meso*-tetra(*para*-chlorophenyl)porphyrin. This is the first example of a hexa-coordinated amino iron(III) porphyrin complex because the reaction of a primary amine with an iron(III) metalloporphyrin leads to the autoreduction of the center metal and a hexa-coordinated iron(II) porphyrin species is formed. The magnetic data are appropriate of a low-spin (S = 1/2) iron(III) metalloporphyrin which is confirmed by the value of the average equatorial distance (Fe—Np) between the central metal and the nitrogen atoms of the porphyrinato ligand. The interactions between the hydrogens of the phenyl group of the trans two 4-ethylaniline axial ligands and the N atoms of the pyrrole of the TClPP moiety are weak compared to the bis(substituted pyridine) iron(III) metallporphyrins leading to a planar porphyrin core with a nearly eclipsed H protons of the 4-ethylaniline ligands and the closest Fe—Np vectors. The planarity of the porphyrin macrocycle is also related to the shift of the $E_{1/2}$[Fe(III)/Fe(II)] of complex (I) toward more negative value. The crystal packing of our iron(III) bis(4-ethyaniline) species is made by a three-dimensional supramolecular structure stabilized by N—H···O and O—H···O hydrogen bonds as well as the non-conventional C—H···O and C—H···Cg intermolecular interactions where Cg is the centroid of a phenyl ring of the 4-ethyaniline axial ligand.

Acknowledgements

The authors gratefully acknowledge financial support from the Ministry of Higher Education and Scientific Research of Tunisia.

Appendix A. Supplementary data

Supplementary data related to this article can be found at https://doi.org/10.1016/j.molstruc.2017.10.023.

References

[1] C.J. Epstein, D.K. Straub, C. Maricondi, Mössbauer spectra of some porphyrin complexes with pyridine, piperidine, and imidazole, Inorg. Chem. 6 (1967) 1720–1724.

[2] D.J. Gaudio, G.N. La Mar, The band structure of the tetracyanoplatinate chain, J. Am. Chem. Soc. 100 (1978) 1112–1119.

[3] C.E. Castro, M. Jamin, W. Yokoyama, R.J. Wade, Ligation and reduction of iron(III) porphyrins by amines. A model for cytochrome P-450 monoamine oxidase, Am. Chem. Soc. 108 (1986) 4179–4187.

[4] O.Q. Munro, P.S. Madlala, R.A.P. Warby, T.B. Seda, G. Hearne, Structural, conformational, and spectroscopic studies of primary amine complexes of iron(II) porphyrins, Inorg. Chem. 38 (1999) 4724–4736.

[5] S. Dhifaoui, W. Harhouri, A. Bujacz, H. Nasri, Crystal structure of bis(benzylamine) [5,10,15,20-tetrakis(4-chlorophenyl)porphyrinato iron(II) n-hexane monosolvate, Acta Cryst. E72 (2016) 102–105.

[6] L.B. Hassen, K. Ezzayani, Y. Rousselin, C. Stern, H. Nasri, C.E. Schulz, Synthesis, UV/vis, FT- IR and Mössbauer spectroscopic characterization and molecular structure of the Bis[4-(2-aminoethyl)morpholine](tetrakis(4-metoxyphenyl) porphyrinato) iron(II) complex, J. Mol. Struct. 1110 (2016) 138–142.

[7] P.J. Marsh, J. Silver, M.C.R. Symons, F.A. Taiwo, Mössbauer and electron paramagnetic resonance studies on some new bis-(ligated) porphyrinato iron(III) complexes with aliphatic amines. Models for cytochromes b, J. Chem. Soc. Dalton Trans. (1996) 2361–2369.

[8] E.S. Schmidt, T.S. Calderwood, T.C. Bruice, Synthesis and characterization of a meso-tetrakis(4- ferrocenylphenyl)porphyrin and examination of its ability to undergo intramolecular photocatalyzed electron transfer, Inorg. Chem. 25 (1986) 3718–6103.

[9] C. Morice, P.L. Maux, G. Simonneaux, Synthesis and characterization of low-spin bis(amino ester) iron(III) porphyrin complexes, Inorg. Chem. 37 (1998) 6100–6103.

[10] M. Kobeissi, L. Oupeth, G. Simonneaux, Synthesis and characterization of low-spin bis(amino ester) iron(III) porphyrin complexes, Acta Cryst. C58 (2002) m443.

[11] S.E. Martinez, D. Huang, A. Szczepaniak, W.A. Cramer, J.L. Smith, Crystal structure of chloroplast cytochrome freveals a novel cytochrome fold and unexpected heme ligation, Structure 2 (1994) 95–105.

[12] A.D. Adler, F.R. Longo, J.D. Finarelli, J. Goldmacher, J. Assour, L.A. Korsakoff, A simplified synthesis for meso-tetraphenylporphine, J. Org. Chem. 32 (1967), 476–476.

[13] J.P. Collman, R.R. Gagne, C. Reed, T.R. Halbert, G. Lang, W.T. Robinson, Picket fence porphyrins. Synthetic models for oxygen binding hemoproteins, J. Am. Chem. Soc. 97 (1975) 1427–1439.

[14] A. Gismelseed, E.L. Bominaar, E. Bill, A.X. Trautwein, H. Winkler, H. Nasri, P. Doppelt, D. Mandon, J. Fischer, R. Weiss, Six-coordinate quantum-mechanically weakley spin-mixed (S = 5/2, 3/2) (triflato)-aquoiron(III) "picket-fence" porphyrin complex: synthesis and structural, Möessbauer, EPR, and magnetic characterization, Inorg. Chem. 92 (1990) 2741–2749.

[15] Earnshaw, Introduction to Magnetochemistry, Academic Press, London, 1968.

[16] R.H. Blessing, Acta.Cryst. A 51 (1995) 33.

[17] A. Altomare, G. Casacarano, C. Giacovazzo, A. Guagliardi, M.C. Burla, G. Polidori, M.J. Camalli, Insights on the uv/vis, fluorescence, and cyclic voltammetry properties and the molecular structures of Zn II tetraphenylporphyrin complexes with pseudohalide axial azido, cyanato- N, thiocyanato- N, and cyanido ligands, Appl. Crystallogr. 27 (1994) 435–436.

[18] G.M. Sheldrick, Acta Cryst. C71 (2015) 3.

[19] W.R. Scheidt, C.A. Reed, Spin-state/stereochemical relationships in iron porphyrins: implications for the hemoproteins, Chem. Rev. 81 (1981) 543–555.

[20] M.E. Kastner, W.R. Scheidt, T. Mashiko, C.A. Reed, Molecular structure of diaquo. alpha, beta, gamma delta tetraphenylporphinatoiron(III) perchlorateandperchlorato-alpha.,beta, gamma,delta-tetraphenylporphinatoiron(III). Two new structural types for iron(III) porphyrins, J. Am. Chem. Soc. 100 (1978) 666–667.

[21] M.K. Safo, G.P. Gupta, F. A.Walker, W.R. Scheidt, Models of the cytochromes b. Control of axial ligand orientation with a hindered porphyrin system, J. Am. Chem. Soc. 113 (1991) 5707–5714.

[22] W.R. Scheidt, Y.J. Lee, Preparation and molecular stereochemistry of anionic difluoro (meso-tetraphenylporphinato)iron(III), a high-spin six-coordinate iron(III) porphyrinate with an unusually expanded core and a hydrogen-bonded "distal" imidazole, J. Am. Chem. Soc. 105 (1983) 778–782.

[23] M. Mylrajan, L.A. Andersson, J. Sun, T.M. Loehr, C.A. Thomas, E.P. Sullivan, M.A. Thomson, K.M. Long, O.P. Anderson, Resonance raman spectroscopic core-size correlations for the crystallogra phically defined complexes Fe^{II}(OEP), Fe^{II}(OEC), Fe^{III}(OEP)(NCS), $[Fe^{III}(OEP)(N\text{-}Melm)_2]^+$, and $[Fe^{III}(OEP)(DMSO)_2]^+$, Inorg. Chem. 34 (1995) 3953–3963.

[24] R. Quinn, C.E. Strouse, J.S. Valentine, Crystal structure and properties of a potassium cryptate salt of bis(4-methylimidazolato)(tetraphenylporphinato) iron(III), Inorg. Chem. 22 (1983) 2934–2940.

[25] D. Inniss, S.M. Soltis, C.E. Strouse, The electronic structure of highly anisotropic low-spin ferric porphyrin complexes based on single-crystal EPR measurements, J. Am. Chem. Soc. 110 (1988) 5644–5650.

[26] M.K. Safo, F.A. Walker, A.M. Raitsimring, W.P. Walters, D.P. Dolata, P.G. Debrunner, W.R Scheidt, Axial ligand orientation in iron(III) porphyrinates; effect of axial π-acceptors. Characterization of the low-spin complex $[Fe(TPP)(4\text{-}CNPy)_2]ClO_4$, J. Am. Chem. Soc. 116 (1994) 7754–7760.

[27] W.R. Scheidt, D.K. Geiger, K.J. Hayes, Control of spin state in (porphinato) iron(III) complexes. An axial ligand orientation effect leading to an intermediate-spin complex. Molecular structure and physical characterization of the monoclinic form of bis(3-chloropyridine)(octaethylporphinato)iron(III) perchlorate, J. Am. Chem. Soc. 104 (1982) 7767–7770.

[28] M.K. Safo, G.P. Gupta, F.A. Walker, W.R. Scheidt, Models of the cytochromes b. Control of axial ligand orientation with a hindered porphyrin system, J. Am. Chem. Soc. 113 (1991) 5497–5510.

[29] S.P. Rath, M.M. Olmstead, A.L. Balch, Electron distribution in iron octaethyloxophlorin complexes. Importance of the Fe(III) oxophlorin trianion form in the bis-pyridine and bis-imidazole complexes, Inorg. Chem. 45 (2006) 6083–6093.

[30] K.M. Kadish, A.B.P. Lever, H.B. Gray, Iron Porphyrin, Part 2, Chap. 4, Addison-Wesley Publishing Company, Massachusetts, 1983.

[31] M.K. Motlagh, M. Noroozifar, J. Saffari, B.O. Patrick, Models of the cytochromes redox properties and jacobson thermodynamic stabilities of complexes of "hindered" iron(III) and iron(II) tetraphenylporphyrinates with substituted pyridines and imidazoles, Inorg. Chim. Acta 362 (2009) 4721–4728.

[32] M.J.M. Nesset, N.V. Shokhirev, P.D. Enemark, S.E. Ann, F. Walker, Models of the cytochromes. Redox properties and thermodynamic stabilities of complexes of "hindered" iron(III) and iron(II) tetraphenylporphyrinates with substituted pyridines and imidazoles, Inorg. Chem. 35 (1996) 5188–5200.

[33] K.M. Kadish, C.H. Su, Relationships between electron-transfer rate constants of bis (ligated)(octaethylporphinato)iron(III) perchlorate and the presence of a spin equilibria, J. Am. Chem. Soc. 105 (1983) 177–180.